

**Long-time relaxation of interacting electrons in the regime of hopping conduction**D. N. Tsigankov,<sup>1</sup> E. Pazy,<sup>2</sup> B. D. Laikhtman,<sup>3</sup> and A. L. Efros<sup>1</sup><sup>1</sup>*Department of Physics, University of Utah, Salt Lake City, Utah 84112, USA*<sup>2</sup>*Department of Physics, Ben-Gurion University of the Negev, Beer-Sheva 84105, Israel*<sup>3</sup>*Department of Physics, Hebrew University, Jerusalem 91904, Israel*

(Received 22 July 2003; revised manuscript received 28 August 2003; published 20 November 2003)

Using numerical simulations we study the long-time relaxation of the hopping conductivity. Even though no modern computation is able to simulate the behavior of a large size system over minutes or hours so as to observe the relaxation, we have been able to show that the long-time relaxation and aging effect observed in experiments can be explained in terms of slow transitions between different pseudo ground states. This was achieved by showing that different pseudoground states may have different conductivities and that the dispersion of conductivities is in agreement with the experimental data. We considered two different two-dimensional models with electron-electron interaction: the lattice model and the random site model, corresponding to “strong” and “weak” effective disorder. For the lattice model, effectively strong disorder, we have shown that the universality of the Coulomb gap, which is responsible for the universal Efros-Shklovskii law for the conductivity, suppresses the long-time relaxation of conductivity since the universality strongly decreases the dispersion of conductivities of the pseudoground states.

DOI: 10.1103/PhysRevB.68.184205

PACS number(s): 71.23.Cq, 72.20.Ee, 72.80.Ng

**I. INTRODUCTION**

The study of electron-electron interactions in the localized regime was initiated by Pollak<sup>1</sup> and Srinivasan.<sup>2</sup> Later, Efros and Shklovskii (ES)<sup>3</sup> showed that the single particle density of states (DOS) tends to zero as the energy tends to the Fermi energy. This phenomenon, called the Coulomb gap, is due to the long-range part of the Coulomb interaction which, in some sense, remains nonscreened. In fact, the Coulomb gap results from the Coulomb law and from the discrete nature of the electron charge. In their first works ES claimed that the DOS in the Coulomb gap has a universal form, depending only on electron charge  $e$  and dielectric constant  $\kappa$ . Then  $\text{DOS} \sim |\varepsilon|^{D-1} \kappa^D / e^{2D}$ , where  $D$  is the spatial dimension and  $\varepsilon$ , is the single-electron energy whose reference point is the chemical potential. This expression for the DOS is the only combination of the energy and the electron charge which has a proper dimensionality. It was shown later<sup>4</sup> that in the two-dimensional (2D) case the above universality is exact only for strong disorder. In the 3D case the question was never studied in detail, however, deviations from the quadratic law have been reported.<sup>5</sup>

Simple quantitative arguments which assume that the single-particle excitations are responsible for the variable range hopping (VRH) lead to the so-called Efros-Shklovskii (ES) law,<sup>3</sup> which has been observed experimentally in many materials

$$\sigma_c \sim (\gamma e^2 / T) \exp[-(T_0 / T)^{1/2}], \quad (1)$$

where  $T$  is the temperature and  $T_0 = \beta_0 e^2 / \kappa a$ ,  $a$  is a localization length of electrons, and  $\kappa$  is an effective dielectric constant of the media above and below 2D gas. A self-consistent type of percolation approach (see references in Ref. 6) gives  $\beta_0 = 6.5$ . The hopping length is given by  $R_C \approx (a/4)(T_0/T)^{1/2}$ .

Recently,<sup>7</sup> using the so-called lattice model, the ES law has been checked in detail by computer simulation. The Hamiltonian of this model is formulated on a square lattice and has a form

$$H = \sum_i \phi_i n_i + \frac{1}{2} \sum_{i \neq j} \frac{(n_i - \nu)(n_j - \nu)}{r_{ij}}, \quad (2)$$

where  $n_i = 0, 1$  are occupation numbers. The quenched random site energies  $\phi_i$  are distributed uniformly within the interval  $[-A, A]$ , where  $A = 1$  is the value employed and the average occupation number  $\nu$  is taken to be  $1/2$ . The magnitude of the quenched disorder is enough so as to provide the universal Coulomb gap at all energies which are important within the temperature range under study.<sup>4</sup> In what follows the lattice constant is taken to be the unit of length. The nearest-neighbor Coulomb energy which is in this case equal to the amplitude of the disorder is considered both as the energy and the temperature unit.

Simulations of the conductivity in the lattice model<sup>7</sup> confirm the ES law in all details, i.e., the pre-exponential factor,  $T$  dependence, and  $a$  dependence. It has also been shown that simultaneous transitions of two electrons do not play any role. Arguments have also been given that any many-electron excitations are not important. Therefore simultaneous transitions of electrons were not included in the simulation below.

Glassy properties, due to both randomness and the long-range Coulomb interaction, are another interesting manifestation of electron-electron interactions in such a system. Davies, Lee, and Rice<sup>8,9</sup> were the first to raise this issue. They coined the phrase “electron glass” which is still used, sometimes also referred to as “Coulomb glass.” Both these terms stress the relation of the above electron system to a spin glass system.

We believe that, in the same way as in real glasses, the glassy properties in this electron system are due to those states which have very close total energies but substantially

different sets of the occupation numbers  $n_i$ . Such states were first observed by Baranovskii *et al.*<sup>10</sup> during the first computer simulation of this system and have been called “pseudo ground states” (PGS’s). These authors found that the PGS’s have the same universal Coulomb gap and have concluded that the existence of PGS’s is not important for the VRH conductivity because transitions between them are very slow. They attributed these slow transitions between the PGS’s as well as their difference from the ground state to be a result of a certain amount of many-electron transitions.

Experiments on the glassy properties of such systems, conducted around 25 years later, have confirmed this conclusion, but they have also shown that Baranovskii *et al.* missed an important feature. Since transitions between PGS’s take a long time and conductivity of these states is not exactly the same, they can serve as a basis for memory effects.

Experiments, started by the group of Ovadyahu<sup>11,12</sup> in 1993, definitely show the relation of this system to the ordinary glasses. In these experiments the difference in the conductivities of the PGS’s is not larger than 10–12%. Similar phenomena was observed by the group of Goldman<sup>13</sup> on ultrathin films of metals near the superconductor-insulator transition. Slow relaxation has been demonstrated by Monroe *et al.*<sup>14</sup> in compensated GaAs.

The properties of the PGS’s have been studied recently, mostly by computational methods.<sup>15–17</sup> Perez-Garrido *et al.*<sup>16</sup> argued that transitions between PGS take a very long time, substantially larger than the time available in any experiment. Menashe *et al.*<sup>17</sup> proposed a different method in order to study the Coulomb glass. By completely ignoring the tunneling term in the transition probability, still keeping the activation probability for the electrons, they performed a thermodynamic Monte Carlo simulation which transforms a nonergodic system into an ergodic one. Thereby they were able to obtain all the thermodynamic properties of the ergodic system since the electrons were able to move across the system in a single transition, leading to effective mixing of all PGS’s.

The above method only permits the calculation of the thermodynamic values, since the number of Monte Carlo steps cannot be related to a physical time. Still, these authors claimed that the metal-insulator transition in the Coulomb glass may coincide with the glassy transition that occurs due to the increase of the localization length. Their method<sup>17</sup> is partially employed in this paper.

The goal of this paper is to understand the origin of the long-time relaxation of conductivity, observed in the experimental papers cited above. To do so we performed Monte Carlo simulations employing the lattice model (2) and the random site model described later on for two-dimensional systems. In our simulation we perturb the system by adding some extra electrons and then trace the relaxation of energy and conductivity with time. One should clearly understand that it is impossible to observe the long-time relaxation by a direct simulation. The general reason for this is due to the long range of the Coulomb interaction and to the fact that in a real sample many transitions take place simultaneously while a computer processor is limited to performing them one at a time as well as updating the resulting changes in the

site energies one at a time. A few additional processors cannot help much. Therefore, even using the most sophisticated program, we may simulate no more than 40  $\mu$ s of the real time in a system of the size of  $100 \times 100$  lattice sites.

We have shown that during such available times we can reach an apparent saturation of conductivity and energy and that saturation of the DOS occurs much earlier. We interpret this “saturation” as a saturation within one PGS. Thus, it is rather the transition from the fast relaxation within one PGS to a very slow relaxation to PGS’s with lower energy, that we cannot observe.

Simultaneously with the conductivity we studied the relaxation of energy. We devised an analytical theory for the energy relaxation which fits the simulation data fairly well and serves as a reference point for our understanding of the short-time relaxation.

To study the long-time relaxation due to transitions between the different PGS’s we came up with a different idea. We create different PGS’s by relaxation from states with different initial distributions of electrons. Then we study the difference between the saturated values of the conductivities of the different PGS’s. If these are different, one should expect that a long-time relaxation exists and the total change of the conductivity should be of the order of this difference. For the lattice model we obtain no such effects. The conductivities of different PGS’s are the same in the limits of our accuracy (about 1–2%).

Since PGS’s with different energies were observed by Menashe *et al.* as well as in other papers, we arrive at the conclusion that the effect of long-time relaxation of the conductivity is absent due to the universality of the Coulomb gap for the lattice model, in the temperature range which we consider. We also performed simulations for the random site model. In this model all disorder comes from the random position of sites. Our results for these simulations exhibit a difference in the conductivities of the PGS’s whose value is sufficiently large so as to explain the experimental results of Ovadyahu’s group.

The difference between these two models in the three-dimensional case has been discussed in Ref. 18. Note that in this case a glassy transition at nonzero temperature has been claimed.<sup>19</sup> Xue and Lee<sup>20</sup> performed Monte Carlo simulations employing the two-dimensional random site model in which the disorder comes about only through the random position of sites. These authors found evidence for glassy behavior at low temperature but they claimed the absence of the glassy transition at nonzero temperature. The same result was obtained for the Ising model.<sup>21</sup>

The paper is organized as follows. In the next section we study the relaxation of the energy and the conductivity after an extra amount of electrons was added to the system in the framework of the lattice model. In Sec. III, employing the lattice model, we study the difference in the conductivities of the PGS’s, obtained through different relaxation methods. In Sec. IV the results for the random site model are presented and discussed.

## II. RELAXATION AFTER ADDITION OF EXTRA ELECTRONS

In this section we study the relaxation of the energy and conductivity of the system after it has been initially per-

turbed by the addition of a few percents of extra electrons. In principle, this is the same procedure employed in the experiments of Ovadyahu's group but the time in which we are able to observe the system is very short. We use the lattice model with Hamiltonian given by Eq. (2) and initial filling factor  $\nu=1/2$ . The extra electrons are added randomly on empty sites and the background is adjusted such that the system remains neutral.

### A. Analytical theory of energy relaxation

To describe the physics of the short-time energy relaxation we devise the following analytical theory. We start by considering a division of a plain containing 2D electrons into regions with a linear size  $R$ . If  $\delta n$  is an average density of additional electrons, the charge  $Q$  of each region is of the order of  $Q \sim e\sqrt{\delta n R^2}$ , because the average charge is compensated by the background. The extra energy due to electron-electron interaction per a region containing excess charge  $Q$  is  $Q^2/R$ . The number of regions per area is  $L^2/R^2$ , where  $L$  is the length of the total system which is square shaped. Thus the extra energy per area due to all regions of size  $R$  is  $\mathcal{E} = e^2 \delta n / \kappa R$ . The regions with the smallest  $R$  give the largest contribution. However, due to relaxation they become neutral faster. So, the main contribution at a time  $t$  comes from the regions in which relaxation has not yet ended. In the 2D case the relaxation goes with the velocity  $\sigma_0/\kappa$ , where  $\sigma_0$  is the conductivity of the system.<sup>22</sup> Thus, at a time  $t$  only the regions with  $R > \sigma_0 t / \kappa$  have an excessive charge. Finally, the energy per area decreases with time as  $\mathcal{E} \sim e^2 \delta n / \sigma_0 t$ . Analyzing results for the autocorrelation functions and density-density correlation functions it is not difficult to find the numerical coefficient in this expression. Let  $n'(\mathbf{r})$  stand for the density of additional electrons with their homogeneous background so that the average value  $\langle n' \rangle$  is zero. The linearized equations have the form

$$\mathbf{j}' = \sigma_0 \mathbf{E} \quad (3)$$

and

$$e \frac{\partial n'}{\partial t} + \sigma_0 \nabla \mathbf{E} = 0. \quad (4)$$

One can see that the diffusion current, omitted here, is more important on the earlier stages of relaxation than the Ohmic current.

In the 3D case the field can be eliminated from these equations resulting in an equation for  $n'$  only. In the 2D case the situation is different and the problem can be solved using the Fourier transformation

$$n' = \frac{1}{L} \sum_{\mathbf{q}} n_{\mathbf{q}} e^{i\mathbf{q} \cdot \mathbf{r}}, \quad \phi = \frac{1}{L} \sum_{\mathbf{q}} \phi_{\mathbf{q}}(z) e^{i\mathbf{q} \cdot \mathbf{r}}. \quad (5)$$

Here  $\mathbf{r}$  and  $\mathbf{q}$  are two-dimensional vectors in the plane of the electrons,  $z$  is the coordinate in the perpendicular direction, and  $\phi$  is the scalar potential. The equation for the potential has the form

$$\frac{d^2 \phi_{\mathbf{q}}}{dz^2} - q^2 \phi_{\mathbf{q}} = - \frac{4\pi e}{\kappa} n_{\mathbf{q}} \delta(z). \quad (6)$$

It can be solved in the regions  $z > 0$  and  $z < 0$ . Under the condition of continuity of  $\phi_{\mathbf{q}}$  at  $z=0$  and zero at  $z \rightarrow \pm \infty$  the solution is

$$\phi_{\mathbf{q}} = A_{\mathbf{q}} e^{-q|z|}. \quad (7)$$

The integration of Eq. (6) over an infinitesimally small interval around  $z=0$  leads to the boundary condition

$$\left. \frac{d\phi_{\mathbf{q}}}{dz} \right|_{z=+0} - \left. \frac{d\phi_{\mathbf{q}}}{dz} \right|_{z=-0} = - \frac{4\pi e}{\kappa} n_{\mathbf{q}}. \quad (8)$$

This condition gives

$$A_{\mathbf{q}} = \frac{2\pi e}{\kappa q} n_{\mathbf{q}}. \quad (9)$$

Equations (7) and (9) give

$$\mathbf{E}_{\mathbf{q}} = -i\mathbf{q} \frac{2\pi e}{\kappa q} n_{\mathbf{q}}, \quad (\nabla \mathbf{E})_{\mathbf{q}} = i\mathbf{q} \cdot \mathbf{E}_{\mathbf{q}} = \frac{2\pi e q}{\kappa} n_{\mathbf{q}}. \quad (10)$$

Now the Fourier transformation of Eq. (4) is

$$\frac{dn_{\mathbf{q}}}{dt} + \frac{n_{\mathbf{q}}}{\tau_{\mathbf{q}}} = 0, \quad (11)$$

where

$$\frac{1}{\tau_{\mathbf{q}}} = \frac{2\pi q}{\kappa} \sigma_0. \quad (12)$$

This leads to

$$n_{\mathbf{q}}(t) = n_{\mathbf{q}}(0) e^{-t/\tau_{\mathbf{q}}}. \quad (13)$$

The energy of the fluctuations is

$$\begin{aligned} \mathcal{E} &= \frac{1}{2} \int \phi(\mathbf{r}, z) e n(\mathbf{r}) \delta(z) d^2 r dz \\ &= \frac{\pi e^2}{\kappa} \int \frac{|n_{\mathbf{q}}(0)|^2}{q} e^{-2t/\tau_{\mathbf{q}}} \frac{d^2 \mathbf{q}}{(2\pi)^2}. \end{aligned} \quad (14)$$

If the initial state corresponds to randomly distributed electrons

$$\langle n'(\mathbf{r}, 0) n'(\mathbf{r}', 0) \rangle = \overline{\Delta n} \delta(\mathbf{r} - \mathbf{r}'), \quad (15)$$

then

$$\begin{aligned} \langle |n_{\mathbf{q}}(0)|^2 \rangle &= \frac{1}{L^2} \left\langle \int e^{i\mathbf{q} \cdot \mathbf{r}} n'(\mathbf{r}, 0) d\mathbf{r} \int e^{-i\mathbf{q} \cdot \mathbf{r}'} n'(\mathbf{r}', 0) d\mathbf{r}' \right\rangle \\ &= \frac{\overline{\Delta n}}{L^2} \int e^{i\mathbf{q} \cdot (\mathbf{r} - \mathbf{r}')} \delta(\mathbf{r} - \mathbf{r}') d\mathbf{r} d\mathbf{r}' = \overline{\Delta n}. \end{aligned} \quad (16)$$

The substitution of Eq. (16) in Eq. (14) gives

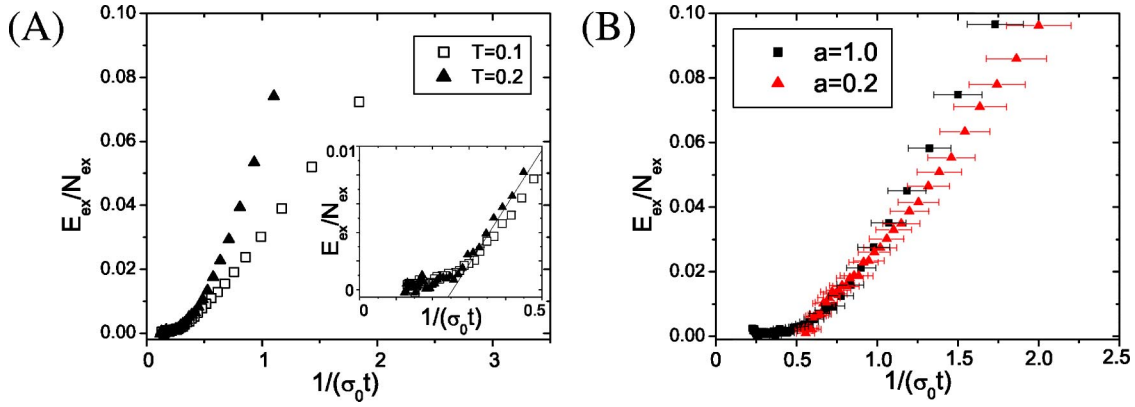


FIG. 1. (a) The time dependence of the total energy of the system is shown at two different temperatures as a function of  $1/\sigma_0 t$ . The localization radius  $a = 1$ , the system size is  $100 \times 100$ . The inset shows the range of time where two curves coincide. The slope, that follows from Eq. (17) is shown by the straight line. All values are given in computer units. (b) The energy relaxation in the VRH ( $a = 1$ ) and in the nearest-neighbor hopping ( $a = 0.2$ ) regimes at  $T = 0.1$ .

$$\mathcal{E} = \frac{\pi e^2 \overline{\Delta n}}{\kappa} \int \frac{1}{q} e^{-2t/\tau_q} \frac{d^2 \mathbf{q}}{(2\pi)^2} = \frac{e^2 \overline{\Delta n}}{8\pi \sigma_0 t}. \quad (17)$$

This result gives the value of the numerical coefficient for the above estimate. One should understand that Eq. (17) is valid at  $t < L/\sigma_0$ . At such times the energy relaxation has finished due to the finite system size. It is easy to take the size effect into account qualitatively. The result is that energy as a function of  $t^{-1}$  saturates at  $t \approx L/\sigma_0$ . It is also important that the system is assumed to be ergodic, i.e., it does not contain different PGS's with slow relaxation between them.

### B. Simulation results for short time relaxation of energy and conductivity

All the time-dependent simulation results in this paper are obtained by our modification of the kinetic Monte Carlo method that is presented in the Appendix. For the lattice model our computer units (CU's) are as follows: the length unit is taken to be the lattice constant  $a_0$ , the units of energy and temperature are given by the Coulomb interaction at the lattice constant  $e^2/a_0$ , the time unit is chosen as the reciprocal transition rate due to phonons  $\gamma^{-1}$ , see Eq. (1), and the unit of the two-dimensional conductivity is given by  $a_0 \gamma$ . The numerical values for the time given below, are calculated using the assumption that  $\gamma = 10^{12} \text{ s}^{-1}$ .

The simulation temperatures were chosen to be  $T = 0.1, 0.2$  which corresponds to the region of hopping conduction in the case were the localization radius  $a$  is of the order of 1 CU.<sup>7</sup> Decreasing the value of  $a$  we may switch from the VRH to the nearest-neighbor hopping regime. The size of the system was taken to be  $100 \times 100$  lattice sites.

The simulation was performed using the following steps: In the first stage the system was brought to "thermal equilibrium," inside a single PGS, using the thermodynamic method employed in the work of Menashe *et al.*<sup>17</sup> In the second stage, which is the reference point for the time from which the relaxation of the DOS starts, energy and conductivity were studied and the electron concentration was slightly changed by adding (or removing) electrons ran-

domly. The time dependencies were averaged over  $10^3$  different sets of randomly distributed extra electrons (holes). Due to electron-hole symmetry of the Hamiltonian (2) at  $\nu = 1/2$  the relaxation of extra electrons and extra holes is the same. The data below describes the addition of electrons. It should be noted that the insertion of electrons into a confined spatial region simulating the way electrons might enter the sample experimentally, or adding electrons to the most probable states. It is clear, however, that since the unperturbed system is saturated within one PGS the difference between different electron insertion scenarios should only be notable within very short time scales, i.e., of the order of our simulation times. Thus the choice of how to simulate the perturbation of the system by adding charge does not in any way effect the long time relaxation of the system which is due to transitions between different PGS's.

The energy relaxation is shown in Fig. 1. The reference point for the total energy  $E_{\text{ex}}$  is the saturated value for the longest time measured. At time  $t = 0$  the filling factor  $\nu$  has been increased from 0.5 to 0.52, such that the total number of extra electrons equals  $N_{\text{ex}} = 0.02L^2/2$ . Figure 1(a) shows the regime of the VRH with  $a = 1$  at two different temperatures. In Figure 1(b) we compare relaxations of energy in the VRH regime at  $a = 1$  with the relaxation in the nearest-neighbor hopping at  $a = 0.2$ . The values of the VRH conductivity at  $a = 1$  are  $\sigma_0 = 0.0048, 0.021$  in CU for  $T = 0.1, 0.2$ , respectively. These values of conductivity are also obtained as the saturated value at the longest time measured. Since Eq. (17) shows that at large  $t$ , the energy  $E$  is a function of  $\sigma_0 t$ , we use this product as a reciprocal argument in Figs. 1, 2. The straight line in the inset of Fig. 1(a) shows the slope as given by Eq. (17). The inset shows the final stage of the relaxation where the curves at different temperatures coincide and obey the time dependence given by Eq. (17). The saturation at even larger  $t$  is due to a size effect. Note that the values of the conductivity  $\sigma_0$  differ by almost five times for the two curves presented. The observed saturation of energy relaxation is connected to the finite size effect as has been discussed in a previous section.

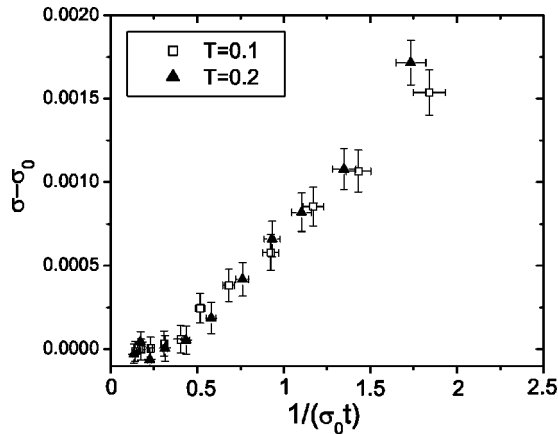


FIG. 2. The time dependence of the conductivity of the system is shown at different temperatures as a function of  $1/\sigma_0 t$ . The value of  $\sigma_0 t$  is taken to be the saturated value of the conductivity at the longest time measured. The concentration changes at  $t=0$  and the parameters of the simulation correspond to those of Fig. 1.

The relaxation of the charge fluctuations given by Eq. (17) not only has the universal form for the different values of conductivities, but it is also independent on the conduction mechanism. In Fig. 1(b) we present the relaxation curves for the system for VRH conductivity and for nearest-neighbor hopping where the localization radius of the electrons is much smaller than the distance between neighboring sites. The time region where the two curves coincide within our accuracy is even broader despite the fact that the values of the conductivity differs by a factor of 3000. The main source of the errors (see the Appendix) arises from calculating the values of the conductivity  $\sigma_0$  rather than measuring the total excessive energy of the system.

Next we present the results for relaxation of the conductivity after adding extra electrons to the system. The procedure for adding the electrons is the same as stated above. The time dependence of the conductivity of the system is shown in Fig. 2 for two different temperatures. These were obtained in the same simulation as the data for the relaxation of the energy in Fig. 1(a). One can see that for both temperatures the conductivity decreases with time finally reaching a kind of saturation, which may also be interpreted as a transition to a substantially slower rate of relaxation. We consider this “saturation” as the end of the short time relaxation in our finite system. The value of the conductivity at the largest time we considered is denoted by  $\sigma_0$ . One can see that as a function of  $1/\sigma_0 t$  the results for both temperatures coincide in an even wider time region than for the total energy of the system. The reason that the conductivity decreases is that, due to the nonequilibrium of the system the extra electrons occupy states above the Fermi level therefore providing higher current than in thermal equilibrium. Note that the saturation of conductivity occurs at the same value of  $\sigma_0 t$ , that is  $\approx 4$  as the saturation of energy. It is reasonable to think that the two processes are connected and the saturation of the conductivity is also a size effect.

The time corresponding to the saturation  $t=4/\sigma_0$  is very short. For  $T=0.1$  and  $a=1$  it is  $\approx 0.8$  ns. Even if we assume

an infinite system and extrapolate the law  $\sigma - \sigma_0 \sim (\sigma_0 t)^{-1}$  to much larger times, we find that in the microsecond range all relaxation which can be observed will be over.

The saturation of the conductivity averaged over different initial distributions of extra electrons, which we have presented in this section, happens at very short times. It is a Maxwell-type relaxation of the extra charge. We have checked that the relaxation of the Coulomb gap inside the energy interval that is responsible for the VRH occurs even faster than the relaxations of the energy and conductivity. These results do not support the idea that long-time relaxation is due to the slow formation of the Coulomb gap.<sup>23</sup>

However in the experimental data<sup>11,12</sup> the long-time relaxation happens on time scales of the order of seconds and hours. These time scales are 9–11 orders of magnitude longer than those which we are able to simulate. Thus, if a long-time relaxation exists in this system, the change of the averaged value of the conductivity is negligible during the physical time scales we have simulated. This explains the apparent saturation of the conductivity, we observe. If the long-time relaxation results from the transitions between different PGS’s, the conductivity we have observed should be considered as the conductivity within a single PGS. The encouraging result obtained in this section is that the saturation of the conductivity of a single PGS can be achieved during the time scale available for our computation. Based on this result another approach to the problem of long-time relaxation, is proposed in the next sections.

### III. CONDUCTIVITY OF DIFFERENT PSEUDO GROUND STATES IN THE LATTICE MODEL

The idea behind our approach is rather simple. We want to compare the conductivity of the system in the different PGS’s. If the values of the obtained conductivities are different for different PGS’s then the long-time relaxation of the conductivity can be attributed to the slow transition between those PGS’s. We are unable to measure time scales of the order of such transitions still we can explain its effect and magnitude which are reflected through the difference in the conductivities of different PGS’s. In the experiments of the group of Ovadyahu<sup>12</sup> such differences are of the order of 10%.

To observe the conductivity of different PGS’s, we measured the conductivity of the same sample with different initial distributions of electrons during the longest time we are able to simulate. The sample is characterized by the total set of random energies  $\phi_i$ . Starting with different initial distributions of electrons the system relaxes to the different PGS’s. If the saturated values of conductivities, measured as in previous section, is different, one should expect that the system will have a long-time relaxation due to transitions between different PGS’s.

The results for the lattice model simulations performed at the lowest available temperature are presented in Fig. 3. The time evolution of the conductivity averaged over the time of measurement is shown for different initial distributions of electrons for the same sample. As one can see there is no appreciable difference in the values of the conductivities

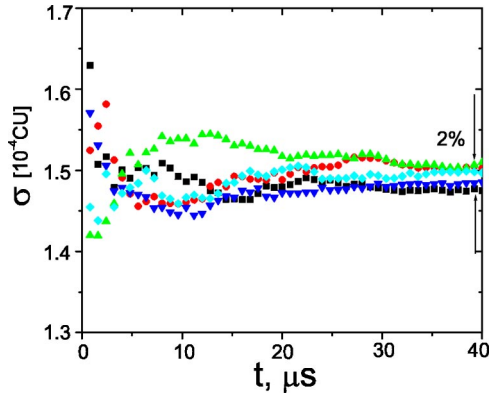


FIG. 3. The time evolution of the conductivity averaged over the time of measurement is shown for different initial distributions of electrons in the lattice model for the same set of  $\phi_i$ . The values of parameters are  $A=1$ ,  $T=0.04$ , the localization radius  $a=1$ , the system size  $L=70$ , and the filling factor  $\nu=1/2$ .

within our accuracy which is about 1–2%. We obtained the same result for all higher temperatures with even greater accuracy.

We therefore conclude that there is no apparent difference in the conductivities of different PGS's for this model down to the lowest temperatures we are able to simulate. We think that the reason for this is the following: It has been shown<sup>7</sup> that the VRH conductivity of the system is provided by the single-electron excitations. The properties of these excitations is defined by the structure of the Coulomb gap. In the lattice model at large  $A$  the DOS in the Coulomb gap has a universal form.<sup>4</sup> It is independent of the properties of the system and is the same for all PGS's. For our temperature range, the case  $A=1$  can be considered as a large disorder. Thus all PGS's have the same conductivities and no long-time relaxation can be observed. We realize that the lattice model with large disorder cannot account for the effect of the long-time relaxation of the conductivity which is observed experimentally. Thus, to observe the difference in the conductivities of different PGS one should take a system with smaller disorder, where the Coulomb gap is not universal. Unfortunately, it is difficult to find such a regime in the lattice model, due to the Wigner crystallization at low temperatures.

#### IV. CONDUCTIVITY OF DIFFERENT PSEUDO GROUND STATES IN THE RANDOM SITE MODEL

In this section we present the results for the random site model. The Hamiltonian of the model has the form

$$H = \frac{1}{2} \sum_{i \neq j} \frac{(n_i - 1/2)(n_j - 1/2)}{r_{ij}}. \quad (18)$$

It differs from Eq. (2) in two important respects. The first, it is formulated on sites  $i, j$ , which have random positions on the plane. The second, any random energies  $\phi_i$ , that are not correlated with the interaction, are absent. Thus, the random positions of the sites is the only source of disorder.

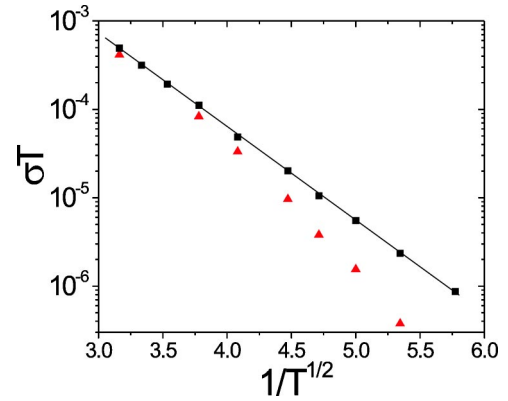


FIG. 4. The temperature dependence of the VRH conductivity in the random site model (triangles) and in the lattice model (squares) is shown. The disorder strength is given by  $A=1$  for the lattice model, while  $A=0$  for the random site model. The localization radius  $a=1$  and the filling factor  $\nu=1/2$ . The straight line represents ES law.

We consider the case  $\nu=1/2$  for which each state of the system has an exact twofold degeneracy: the total energy is invariant with respect to changing all of the occupation numbers  $n_i \rightarrow 1 - n_i$ . It is this symmetry for half filling which allows this model to be mapped on to a spin glass model.<sup>19</sup> This fact is probably also important for formation of PGS that consist of fragments of both states.

This model is unusual for electronic systems. For example, partially occupied donors located in a plane with a gate electrode above the plane are not described by this model. In this case the above symmetry is absent. However, the neutral system of random donors with a large “negative  $U$ ” can be described by the Hamiltonian (18), if 1/2 of them are doubly occupied with charge  $-1$  and the other half are not occupied with the charge 1.

For the simulation of the random site model we use a similar computational algorithm which is described in the Appendix. Unfortunately, it is more time and memory consuming than the algorithm for the lattice model. In this model the unit of length is  $a_0 = n^{-1/2}$ , where  $n$  is the concentration of sites.

Figure 4 shows the temperature dependences of the VRH conductivities both in the random site model and in the lattice model. Unfortunately for the random site model we were unable to check the importance of simultaneous many-electron transitions on the VRH conductivity. One can see a deviation from the ES law in the case of the random site model that might be a result of deviation of the DOS from the universal DOS in the Coulomb gap.

Figure 5 confirms this point of view. It shows the DOS of different PGS's for both lattice and random site models. As in the previous section the different PGS's have been obtained by simulations starting from different initial distribution of electrons but with the same disorder. The latter condition means the same set of  $\phi_i$  or the same set of random sites depending on the model. In each case the DOS is calculated by two methods. The first is the kinetic Monte Carlo method, which gives the DOS in one PGS due to the time constraint and the second is the thermodynamic Monte Carlo

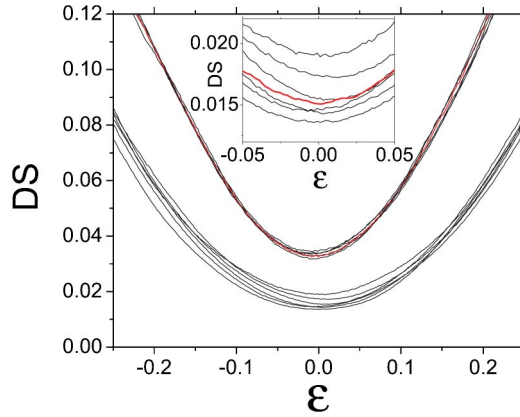


FIG. 5. The DOS in the vicinity of the Fermi level at  $T=0.04$  as a function of the single-particle energy  $\varepsilon$  with a reference point at the Fermi level is shown for the lattice model (the upper set of curves) and random site model (lower curves) is presented for five different initial distributions of electrons for each model. The DOS is averaged over a time equal to  $1 \mu\text{s}$ . The inset shows the DOS, near the Fermi level, for the random site model in an enlarged scale. The thermodynamic DOS is emphasized in the inset by a thick line. The values for the parameters used to obtain these curves are the same as were employed in Fig. 4.

method which gives the DOS averaged over all PGS's. To get to the thermodynamic regime one should ignore the tunneling exponent in the transition rate so that transition at any distance becomes possible. However, the energy dependence of the rate should be strictly preserved to get the correct ergodic thermodynamic result. Menashe *et al.*<sup>17</sup> have shown that this method provides an effective thermalization including fast transitions between the PGS's.

Figure 5 contains two important results. (i) The DOS of the random site model strongly differs from the DOS of the lattice model and does not have the standard energy dependence typical for the two-dimensional Coulomb gap, which is known to be very robust in the lattice model for  $A=1$ . For the random site model the DOS is quadratic rather than linear. We have checked that its curvature is  $T$  independent. From dimensionality considerations this DOS can only be of the order of  $\varepsilon^2/e^6 n^{1/2}$ , which also explains the deviation from the ES law for the VRH conductivity shown in Fig. 4. (ii) The relative difference between the DOS for different PGS's is much larger for the random site model than for the lattice model. For the random site model the time fluctuations of DOS near the Fermi level are 10 times smaller than the difference between the DOS's of different PGS's. In the lattice model those fluctuations are so close to the difference itself that the difference is not a reliable measure. The thermodynamic DOS is between the DOS's obtained for different PGS's as it should be for an average function.

In fact results (i) and (ii) are connected to each other. At large  $A$  the universal behavior of the Coulomb gap can be obtained from conditions  $\varepsilon_j - \varepsilon_i - 1/r_{ij} > 0$  for every empty site  $j$  and occupied site  $i$ . These conditions are important near the Fermi energy only, for which the total energy becomes irrelevant. That is the reason why all PGS's have a similar DOS near the Fermi level. For the random site model these

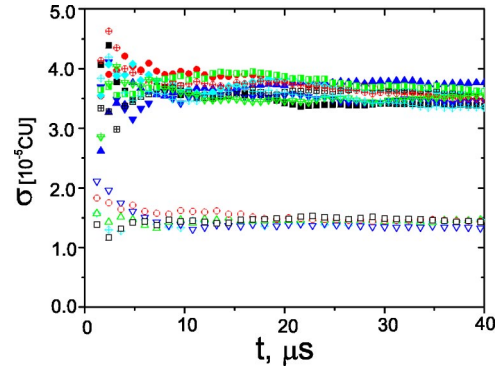


FIG. 6. The time evolution of the conductivities of different PGS's for the model with the random site distribution are shown by filled symbols. Open symbols show the same evolution for a "compound" system with  $A=1$ . The values of parameters  $T=0.04$ , localization radius  $a=1$ , the system size  $L=70$ , and the filling factor  $\nu=1/2$ .

conditions are also necessary but there should be some other restrictions that make the DOS smaller. Those restrictions should be connected with the average distance between the sites and therefore they are related to the total energy. Therefore it is interesting to study the conductivity of different PGS's in this model.

The simulation results for the time evolution of the conductivities of different PGS's for the model with the random spatial site distribution are shown in Fig. 6 by filled symbols at the same temperature as for the lattice model. In this case the conductivity value of each individual PGS saturates within 1% during the time of the simulation. However, the saturated values of the conductivities differ by 12% for the different initial distributions of electrons in the same sample. This is by an order of magnitude greater than the simulation accuracy. The study of the conductivities in the random site model shows that the slow transitions between PGS's may result in the long-time relaxation of the conductivity observed in the experiment. An important question now is whether the obtained result is due to the randomness in the site distribution or to the absence of the disorder which is not correlated with the interaction.

In order to answer this question we consider a "compound" model. Namely, we have added to the Hamiltonian of the random site model (18) the first term in Eq. (2) with  $A=1$ . One can see from Fig. 6 that the difference in the conductivities of different PGS's disappears at  $A=1$  within the simulation accuracy. Thus, the randomness of the sites is not important, but the value of  $A$  is very important.

Another important question is whether the values of the conductivity of the different PGS's are correlated with the energies of these PGS's. The total energy of the system in a given PGS is averaged over time and plotted versus the value of the conductivity for the same PGS's in Fig. 7. The data shows that the energy dependence of the conductivity is close to a linear behavior. PGS's with higher average total energy also have a larger value for the conductivity which is reasonable, since in the states with lower energy the electrons are in positions where they are more tightly bound and therefore their conductivity is lower. The same behavior is

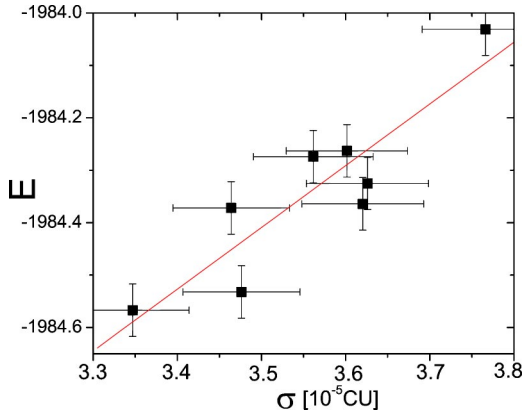


FIG. 7. The correlation between the total energy of the system and the conductivity is shown for eight different initial distributions of electrons in the random site model. Both the total energy and the conductivity are averaged over the time  $40 \mu\text{s}$ . The straight line is given as a guide for the eye. The values of the parameters used are the same as were used in Fig. 6.

apparent in the experimental results of Ovadyahu.<sup>12</sup> The linear dependence is also reasonable because the energy difference between PGS's is small and conductivity as a function of energy may be expanded into a Taylor series, taking the first term. Similar to Anderson *et al.*<sup>24</sup> one can show that the possibility of the Taylor expansion leads to the relaxation laws  $\delta E \sim -\ln t$  and  $\delta \sigma \sim -\ln t$ .

## V. CONCLUSIONS

A computational algorithm is presented which permits one to simulate the energy, density of states, and conductivity of a system with localized interacting electrons during times of the order of  $40 \mu\text{s}$ . We argue that during this time the relaxation of the system to some PGS's is completed. An analytical theory of the energy relaxation which is in good agreement with the computational data is presented. Our computational results for the conductivity exhibit two very distinct time scales: the first is a very short time scale corresponding to the average value of the conductivity, the second a very long time scale defined by the long-time relaxation of the conductivity. We attribute these two scales to the following physical picture, in which the relatively short time scale is a consequence of the relaxation of the system within one PGS, well described by our analytical theory, as well as by our simulations, whereas the long-time relaxation of the conductivity, is related to transitions between different PGS's. The microscopic origin of this huge time scale separation can be attributed to the fact that whereas many-electron transitions are not important for the VRH conductivity within one PGS they play an important role in slowing down transitions between PGS's.

Current computational resources are not able to confirm this theory by directly observing the long relaxation processes, rather they are limited to the range of the short relaxation time scales, which can be simulated. In order to check our theory we have studied the conductivities of the different PGS's to see whether or not they are different. We employed

two different models: the lattice model and the random site model, with random sites and no external disorder. We have shown that these two different models which correspond to different realizations of disorder lead to different physical effects. For the lattice model no difference in the conductivities of the different PGS's was found. We understand this result in terms of universality of the Coulomb gap and ES hopping conduction.

For the model with random distances between sites and no external disorder we have found the difference of the conductivities to be within 10–12 % which is large enough to explain the experimental data. We have also shown that the density of states in this model is not universal and that hopping conductivity does not obey the ES law. We think that similar effects might be observed in the lattice model as well with  $A = 1$  but at lower temperatures than those which we are able to simulate. With increasing  $A$  this temperature range should become lower. Thus we think that the universality of the Coulomb gap that manifests itself in the ES law for the VRH suppresses the long-time relaxation because in this case, the conductivities of PGS's are very close to each other.

## ACKNOWLEDGMENTS

The work has been funded by the US-Israel Binational Science Foundation Grant No. 9800097. The computations have been made at the CHPC of the University of Utah. A.E. is grateful to the Aspen Center for Physics, where this paper was presented for the first time, and to Boris Shklovskii and Zvi Ovadyahu for important comments.

## APPENDIX: COMPUTATIONAL ALGORITHM

To perform the simulation of the transport and thermodynamic properties on the finite array  $L \times L$  for both the lattice model and the model with random spatial site distribution we use the periodic boundary conditions on a torus. In fact, this means that for the pair of sites  $i$  and  $j$  the distance between them is given by  $r_{ij} = [(\Delta x_{ij})^2 + (\Delta y_{ij})^2]^{1/2}$ , where

$$\begin{aligned} \Delta x_{ij} &= \min(|x_i - x_j|, L - |x_i - x_j|) \Delta y_{ij} \\ &= \min(|y_i - y_j|, L - |y_i - y_j|). \end{aligned} \quad (\text{A1})$$

Here  $x_i$  and  $y_i$  are the sets of the site coordinates, which form a lattice in one model and are random in the other.

To simulate the conductivity one should add a term  $\sum_i E x_i$  to the Hamiltonian (2) where  $E$  is a weak electric field. Due to the field the current flows around the torus in the  $x$  direction. It is convenient to calculate the total dipole moment due to electron transitions in the direction of the electric field and obtain the conductivity from the equation

$$\sigma = \frac{1}{EL^2} \frac{dP}{dt}. \quad (\text{A2})$$

On average the dipole moment  $P$  increases linearly with time.

To find  $dP/dt$  one needs a kinetic Monte Carlo (MC) algorithm that connects the number of MC steps with a real

time  $t$ . Note that for any thermodynamic calculation the time is irrelevant. The starting equation is a transition rate for a single electron hop from site  $i$  to site  $j$ , that has the form

$$\Gamma_{ij} = \gamma \theta_{ij} \frac{\exp(-2r_{ij}/a)}{1 + \exp(\varepsilon_{ij}/T)}, \quad (\text{A3})$$

where  $r_{ij}$  is the distance between the sites  $i$  and  $j$ ,  $\varepsilon_{ij}$  is the energy difference between the two configurations  $\varepsilon_{ij} = \varepsilon_i - \varepsilon_j - 1/r_{ij} - E\Delta x_{ij}$ ,  $\varepsilon_i = \phi_i + \sum_j (1/r_{ij})(n_j - \nu)$ ,  $\Delta x_{ij}$  is given by Eq. (A1), and  $\theta_{ij}$  is equal to 1 if the site  $i$  is occupied and site  $j$  is empty or 0 otherwise. The transition rate should have the dimensionality of frequency. It is written in a dimensionless form, assuming that our time unit is  $\gamma^{-1}$ . The MC process can be started with any initial set of distributions for the occupation numbers  $n_i$  which evolves during the simulation.

There are two different algorithms developed for this type of computer simulation. The first one implies the calculation of all the transition rates  $\Gamma_{ij}$  in the system at each Monte Carlo (MC) step. Then the probability that the next transition to occur  $i \rightarrow j$  is given by

$$\frac{\Gamma_{ij}}{\sum_i \sum_{j \neq i} \Gamma_{ij}}. \quad (\text{A4})$$

Then at each MC step the code chooses the transition with the above probability and performs it. This means changing the occupation numbers  $n_i$  and  $n_j$ , calculating the contribution of this transition into the total dipole moment  $P$ , and recalculating all site energies and transition rates. After that the code comes to the next MC step.

For the above algorithm the physical time  $\Delta t$  for each MC step is

$$\Delta t = \left( \sum_i \sum_{j \neq i} \Gamma_{ij} \right)^{-1}, \quad (\text{A5})$$

because in the real system all processes run simultaneously. Note, that  $\Delta t$  depends on the configuration of the system and varies during the simulation.

In the second algorithm at each MC step a pair of sites  $(i, j)$  is chosen with equal probability from all possible sets. Then the transition  $(i \rightarrow j)$  is accepted with the probability  $\Gamma_{ij}$ . If the transition is rejected, the MC step is over and the code proceeds to the next MC step. If it is accepted, the transition is performed. This means that the code changes occupation numbers  $n_i$  and  $n_j$ , calculates the contribution of this transition into the total dipole moment  $P$ , and recalculates all the site energies  $\varepsilon_{ij}$ . This is the end of the MC step. In this case, the physical time per one MC step is constant and equal to

$$\Delta t = \frac{1}{N_{\text{tr}}} = \frac{1}{L^2(L^2 - 1)}, \quad (\text{A6})$$

$\Delta t = 1/N_{\text{tr}}$ , where  $N_{\text{tr}}$  is the total number of different transitions in the system.

The advantage of the first algorithm is that any MC step is successful: as a result of each step one electron moves from one site to another. The disadvantage is that for the interacting systems at each MC step the computer recalculates  $N_{\text{tr}}$  values of  $\Gamma_{ij}$ . Therefore, each MC step is very time consuming as compared to the MC step of the second algorithm. However, the disadvantage of the second algorithm is that at strong dispersion of the transition rates (small  $a$  or  $T$ ) the probability of the rejection is very high. In other words, the physical time  $\Delta t$  per one MC step is much smaller than in the first algorithm. This can be seen from Eqs. (A5), (A6). Indeed, the double sum in Eq. (A5) contains  $N_{\text{tr}}$  terms. However, the majority of these terms are very small.

In this paper, we used a mixed scheme which combines the best features of both algorithms discussed above. We show that it is very efficient in the VRH regime for the interacting electrons. The original idea for this algorithm belongs to Biham.<sup>25</sup>

The transition rate (A3) for the VRH can be written as a product  $\Gamma_{ij}^T \Gamma_{ij}^A$ , where the ‘‘tunneling’’ part of the transition rate  $\Gamma_{ij}^T = \exp(-2r_{ij}/a)$ , while  $\Gamma_{ij}^A = \theta_{ij}/[1 + \exp(\varepsilon_{ij}/T)]$  reflects activation. It is important now that  $\Gamma^T$  is independent of the configurations of electrons and should be calculated only once. Since the probabilities of tunneling and activation are independent we may apply the first algorithm with  $\Gamma^T$  and the second one with  $\Gamma^A$ . Practically it means that we choose pairs  $(i, j)$  with the probabilities

$$\frac{\Gamma_{ij}^T}{\sum_i \sum_{j \neq i} \Gamma_{ij}^T} \quad (\text{A7})$$

and accept the transition  $i \rightarrow j$  with the probability  $\theta_{ij}/[1 + \exp(\varepsilon_{ij}/T)]$ . If the transition is rejected then the MC step is over and the code proceeds to the next MC step. If it is accepted, the transition is performed. To finish this step the code changes the occupation numbers  $n_i$  and  $n_j$ , calculates the contribution of this transition into the total dipole moment  $P$ , and recalculates all the site energies  $\varepsilon_i$ . In this case, the physical time per one MC step is constant and equal to

$$\Delta t = \left( \sum_i \sum_{j \neq i} \Gamma_{ij}^T \right)^{-1}. \quad (\text{A8})$$

For the lattice model the sum  $\sum_{j \neq i} \Gamma_{ij}^T$  is independent on  $i$  thus  $\Delta t = (L^2 \sum_{j \neq i} \Gamma_{ij}^T)^{-1}$ . Using this result the conductivity in units of  $\gamma a_0$  can be written in the form

$$\sigma = \frac{1}{EL^2} \frac{dP}{dt} = \frac{P \sum_{j \neq i} \exp(-2r_{ij}/a)}{EN_{\text{MC}}}, \quad (\text{A9})$$

where  $P$  is the total dipole moment due to the electron transitions after  $N_{\text{MC}}$  steps.

For the model with random spatial site distribution the  $\sum_{j \neq i} \Gamma_{ij}^T$  is different for each site  $i$  and the conductivity is given by

TABLE I. The algorithm efficiency comparison.

Algorithm	$\Delta t^{-1}$	$N_{\text{oper}}/N_{\text{MC}}$	Eff [oper/sec]
I	$O(N)$	$O(N^2)$	$O(N^3)$
II	$O(N^2)$	$O(N)$	$O(N^3)$
Mixed	$O(N)$	$O(N)$	$O(N^2)$

$$\sigma = \frac{P \sum_i \sum_{j \neq i} \exp(-2r_{ij}/a)}{EN_{\text{MC}}L^2}. \quad (\text{A10})$$

Now we compare the efficiency of all three algorithms. The efficiency is the number of operations which are necessary to simulate a physical process during a time  $t$ . The most important is how the efficiency depends on the number of sites in the system  $N=L^2$ . The results are shown in Table I. In the

table  $\Delta t$  is the physical time correspondent to one MC step,  $N_{\text{OP}}/N_{\text{MC}}$  is the number of operations per MC step, and the efficiency is given by  $\text{Eff} = N_{\text{OP}}/N_{\text{MC}}\Delta t$ .

The time efficiency of the mixed algorithm is the same for both lattice and random site models. However, the memory requirements are much harder for the random site model. In this model one need to calculate all  $N^2=L^4$  tunneling terms and have access to all of them at each MC step, because the transition at each step is chosen with the above weights. While in the lattice model there is only  $N=L^2$  different tunneling terms  $\exp(-2r_{ij}/a)$  that have to be stored. In fact, this constraint does not allow us to simulate a system in which the number of sites exceeds 5000 employing the random site model.

One can see from Table I that the efficiency of the mixed algorithm is the best. The use of this algorithm allowed us to simulate the macroscopic conductivity. In fact this algorithm has been used in Ref. 7.

- 
- <sup>1</sup>M. Pollak, Discuss. Faraday Soc. **50**, 13 (1970).  
<sup>2</sup>G. Srinivasan, Phys. Rev. B **4**, 2581 (1971).  
<sup>3</sup>A.L. Efros and B.I. Shklovskii, J. Phys. C **8**, L49 (1975).  
<sup>4</sup>F.G. Pikus and A.L. Efros, Phys. Rev. Lett. **73**, 3014 (1994).  
<sup>5</sup>A. Mobius, M. Richter, and B. Drittler, Phys. Rev. B **45**, 11 568 (1992).  
<sup>6</sup>E.I. Levin, V.L. Nguen, B.I. Shklovskii, and A.L. Efros, Sov. Phys. JETP **85**, 842 (1987).  
<sup>7</sup>D.N. Tsiganov and A.L. Efros, Phys. Rev. Lett. **88**, 176602 (2002).  
<sup>8</sup>J.H. Davies, P.A. Lee, and T.M. Rice, Phys. Rev. Lett. **49**, 758 (1982).  
<sup>9</sup>J.H. Davies, P.A. Lee, and T.M. Rice, Phys. Rev. B **29**, 4260 (1984).  
<sup>10</sup>S.D. Baranovskii, A.L. Efros, B.L. Gelmont, and B.I. Shklovskii, J. Phys. C **12**, 1023 (1979).  
<sup>11</sup>M. Ben-Chorin, Z. Ovadyahu, and M. Pollak, Phys. Rev. B **48**, 15 025 (1993).  
<sup>12</sup>A. Vakhin, Z. Ovadyahu, and M. Pollak, Phys. Rev. Lett. **84**, 3402 (2000).  
<sup>13</sup>G. Martinez-Arizala, D.E. Grupp, C. Christiansen, A.M. Mack, N. Markovic, Y. Seguchi, and A.M. Goldman, Phys. Rev. Lett. **78**, 1130 (1997).  
<sup>14</sup>D. Monroe, A.C. Gossard, J.H. English, B. Golding, W.H. Haemmerle, and M.A. Kastner, Phys. Rev. Lett. **59**, 1148 (1987).  
<sup>15</sup>Sh. Kogan, Phys. Rev. B **57**, 9736 (1998).  
<sup>16</sup>A. Perez-Garrido, M. Ortuno, and A. Diaz-Sanches, Phys. Status Solidi B **205**, 31 (1998).  
<sup>17</sup>D. Menashe, O. Biham, B.D. Laikhtman, and A.L. Efros, Phys. Rev. B **64**, 115209 (2001).  
<sup>18</sup>T. Vojta and M. Schreiber, Phys. Rev. Lett. **73**, 2933 (1994); E.R. Grannan and C.C. Yu, *ibid.* **73**, 2934 (1994).  
<sup>19</sup>E.R. Grannan and C.C. Yu, Phys. Rev. Lett. **71**, 3335 (1993).  
<sup>20</sup>W. Xue and P.A. Lee, Phys. Rev. B **38**, 9093 (1988).  
<sup>21</sup>K. Binder and A.P. Young, Rev. Mod. Phys. **58**, 801 (1986).  
<sup>22</sup>M.I. Dyakonov and A.S. Furman, Sov. Phys. JETP **65**, 574 (1987).  
<sup>23</sup>C.C. Yu, Phys. Rev. Lett. **82**, 4074 (1999).  
<sup>24</sup>P.W. Anderson, B.I. Halperin, and C.M. Varma, Philos. Mag. **25**, 1 (1972).  
<sup>25</sup>O. Biham (private communication).